energies

MDPI

Article

Accelerating Optimal Control Strategy Generation for HVAC Systems Using a Scenario Reduction Method: A Case Study

Zhe Tian [1,2], Chuang Ye [1], Jie Zhu [1], Jide Niu [1,2,*] and Yakai Lu [3]

[1] School of Environmental Science and Engineering, Tianjin University, Tianjin 300072, China
[2] Tianjin Key Laboratory of Building Environment and Energy, Tianjin 300072, China
[3] School of Energy and Environmental Engineering, Hebei University of Technology, Tianjin 300401, China
* Correspondence: niujide@tju.edu.cn

Abstract: Learning an optimal control strategy from the optimized operating dataset is a feasible way to improve the operational efficiency of HVAC systems. The operation dataset is the key to ensuring the global optimality and universality of the operation strategy. Currently, the model-based method is commonly used to generate datasets that cover all operating scenarios throughout the cooling season. However, thousands of iterative optimizations of the model also lead to high computational costs. Therefore, this paper proposed a scenario reduction method in which similar operating scenarios were grouped into clusters to significantly reduce the number of optimization calculations. First, k-means clustering (with dry-bulb temperature, wet-bulb temperature, and cooling load as features) was used to select typical scenarios from operating scenarios for the entire cooling season. Second, the model-based optimization was performed with the typical scenarios to generate the optimal operating dataset. Taking a railway station in Beijing as a case study, the results show that the optimization time for the typical scenarios was only 1.4 days, which was reduced by 93.1% compared with the 20.6 days required to optimize the complete cooling season scenario. The optimal control rules were extracted, respectively, from the above datasets generated under the two schemes, and the results show that the deviation of energy saving rate was only 0.45%. This study shows that the scenario reduction method can significantly speed up the generation of the optimal control strategy dataset while ensuring the energy-saving effect.

Keywords: HVAC system; offline optimization; rule-based control; scenario reduction; clustering

Citation: Tian, Z.; Ye, C.; Zhu, J.; Niu, J.; Lu, Y. Accelerating Optimal Control Strategy Generation for HVAC Systems Using a Scenario Reduction Method: A Case Study. *Energies* **2023**, *16*, 2988. https://doi.org/10.3390/en16072988

Academic Editor: Francesco Nocera

Received: 8 March 2023
Revised: 18 March 2023
Accepted: 22 March 2023
Published: 24 March 2023

1. Introduction

Globally, buildings consume about 36% of the total energy [1], while most of the energy consumption in buildings comes from space heating, cooling, or ventilating systems [2]. Data show that the energy consumption of HVAC systems will continue to grow with climate deterioration and people's increasing demand for a better indoor environment [3]. Therefore, under the policy of promoting energy conservation and emission reduction, the optimal operation of HVAC systems has become the focus of many researchers. In these studies, the model-based control (MBC) method has received more and more attention [4–8]. In this method, building energy simulation (BES) programs and optimization technologies are combined to guide the operation of HVAC systems [8]. Good results were achieved in various cases using this method, with an average energy-saving rate of up to 13–28% [9–14].

However, in practical use, such a method often carries a sizeable mathematical calculation burden. On the one hand, an HVAC system contains multiple optimization setpoints, including discrete ones (e.g., the number of chillers in operation) and continuous ones (e.g., the temperature setpoints) [8]. On the other hand, within the model of an HVAC system, there tends to be a mass of complex mechanism descriptions and nonlinear processes [4,15]. As a result, online optimal control of HVAC systems is often challenging to implement due to its high burden on optimization calculation. Additionally, the control

algorithm is hard to implement in high-level languages for most automatic control systems in practice due to their hardware limitations, increasing the difficulty of deploying real-time optimization. To solve the problems mentioned above, researchers try to optimize beforehand [16–19]: (i) obtain training dataset containing information about the optimal control strategy through virtual operation optimization (later on, we will use the term training dataset to simplify the presentation) and (ii) extract the rule-based strategies from the training dataset to support the online operation of the HVAC system. In this way, optimization calculation is not required during the system operation stage, and the strategies in the form of formulae are easier to deploy in the industrial low-power control hardware.

As the rule-based strategies are derived from the optimal control strategy dataset, the effect of using these rule-based strategies is determined by the completeness of the operation scenarios covered by the dataset. In other words, the accuracy of these rule-based strategies will be damaged when the actual operating conditions are beyond the scope of the set. To avoid this problem, enormous operation scenarios are required for the offline optimization scheme, leading to a long cycle for strategy set formulation. For instance, in ref. [20], it took 12 h in total (Virtual run time of 11 weeks) to obtain data that reflect the window's on/off control strategy of the window. This duration would climb with more control variables and an extended operation period. In this case, technicians have to wait a long time to do the following work, which could not be conducive to formulating or updating strategies. So, this paper attempts to improve the offline optimization scheme and proposes a more efficient method to obtain the training dataset.

Methods for improving the efficiency of generating the training dataset can be divided into two categories. For the first category, the computational efficiency is improved by augmenting the calculation speed of the model. Although models generated by traditional building energy simulation (BES) programs have good generalization performance [20], their complex formulae restrict the calculation speed and thus hinder the solution of subsequent optimization problems [5,21]. For this reason, researchers tried to simplify the mechanism model in some appropriate ways [22]. For instance, Haves et al. reduced the number of dynamic states for the tank model to three by simplifying thermocline in the energy storage tank so that the calculation burden was decreased [12]; Picard et al. proposed a method to obtain the linear state space model based on the BES program, and the calculation speed was 8.5 times faster [15]. By simplifying the model, these studies accelerated the calculation speed. However, this came at the cost of sacrificing the model's accuracy to some extent [15], and the balance between speed and accuracy determined the effectiveness of this approach. In addition, using data-driven models with faster calculation speed is also an effective way [23,24]. For example, Afroz et al. used the neural network model to describe the relation between setpoints, energy consumption, and environmental parameters [25]; Magnier et al. modeled with artificial neural networks and completed the optimization in three weeks [26]. Data-driven models have brought fast calculation speed; however, the broader application of data-driven models is limited due to the requirements for large amounts of training data and the uncertainty of calculation results [4,27].

For the second category, optimization algorithms are improved for higher computational efficiency [28,29]. Due to the limitations of traditional BES modeling tools, obtaining the objective function's gradient is often difficult. Therefore, in some studies, improvements were made based on heuristic algorithms [30–33]. For example, Huang et al. improved the way of selecting the start point of the optimization [11]; Sun et al. added the equilibrium optimization algorithm into the HVAC system to achieve faster calculation speed and better results [30]. Other studies gave up traditional modeling tools for more efficient algorithms [34–36]. For instance, Kusiak combined the data-driven model with the interior-point method and solved the computational problem of optimization [34]; Castilla linearized the model so that the Quadratic Programming algorithm could be applied to reduce the computational burden of optimization [35]; Åkesson developed Jmodelica, and it can satisfy users' needs for different algorithms [36]. Unfortunately, most such tools are

just for research and require multidisciplinary expertise, making it difficult to improve the algorithms [5,8].

Nevertheless, from the perspective of training dataset acquisition, the efficiency of obtaining the optimal control strategy dataset cannot be entirely augmented by regulating models and algorithms because the quality of models and algorithms only affects the computational speed of a single optimization process, while the number of virtual operation scenarios determines the number of optimization processes needs to be executed. Therefore, how to construct the virtual operation scenarios to be optimized is also essential for improving the efficiency of generating and obtaining the training dataset.

Generally, there are two ways of constructing the virtual operation scenarios to be optimized. One is to simulate the HVAC system throughout the cooling season, and the collection of simulated operation scenarios in time series is taken as the set to be optimized [37]. The other is to generate the grid of operation scenarios via orthogonality [38]. For the former, there are numerous similar scenarios in the simulated set (for example, the meteorology and the cooling load on successive days do not differ significantly). These scenarios are different, but slight differences do not necessarily lead to discrepancies in the value of optimal setpoints. Hence, similar scenarios can be deleted appropriately to ease the computational burden of optimization. For the latter, with the increase in parameters used to describe the scenarios, the number of virtual operation scenarios will significantly grow, which can even lead to the failure of this method [19]. An actual operation scenario of an HVAC system contains both meteorological parameters and cooling load related parameters, and the two are correlated in a certain way (higher outdoor temperature often means more cooling load). However, the latter method (to generate the grid of operation scenarios via orthogonality) ignores such correlation. It performs invalid optimization in some unrealistic scenarios, resulting in a loss of computational efficiency.

Given the drawbacks of existing methods, this paper proposes a framework for constructing the training dataset to improve the efficiency of generating optimal control strategies. Firstly, a method for constructing typical operation scenarios was proposed to avoid invalid optimization in the offline rule-based strategy generation, thus improving the computational efficiency. In this method, we first obtain the HVAC system operation scenarios in time series based on simulation to obtain the characteristics of the actual operation scenarios of the system. Then we use the clustering technique to exclude similar scenarios among them and reduce the appearance of similar scenarios. Secondly, we integrated the method into Coffey's offline optimization framework [38], and took a high-speed railway station in Beijing as a case study to verify the method's effectiveness in the simulation platform. Additionally, we quantified the effect of the number of clusters and evaluated the correspondence between the implementation effect of the strategies and the proposed verification indicators, and this provided guidelines for determining the number of clusters.

The organization of this article is as follows: in Section 2, an efficient method for obtaining the training dataset based on boundary scenario reduction is introduced, including the methods for acquiring typical operation scenarios and evaluating the training dataset. In Section 3, a model-based optimization implementation framework and a lookup table-based offline optimization approach are presented as validation frameworks. In Section 4, the study case is described, and the experimental design for the control group is explained. In Section 5, the results and discussions of different schemes are presented and analyzed. Finally, the conclusion and prospects are presented in Section 6, describing the applicability of the proposed framework and the direction for future work.

2. Method for Constructing Training Dataset

To illustrate the method more clearly, we took a common HVAC system as the research object, which is shown in Figure 1. All devices in the system are equipped with frequency converters, which ensures the implementation of optimal operation. The time constant of this system is small due to the lack of energy storage devices. As a result, changes in the operating conditions scenario at one point do not affect the system operation at other times.

Therefore, when generating the optimal control strategies at the current point, the influence of operation conditions scenarios at other times does not need to be considered. In this way, the optimization process is simplified, making it easier to elaborate the idea of this paper.

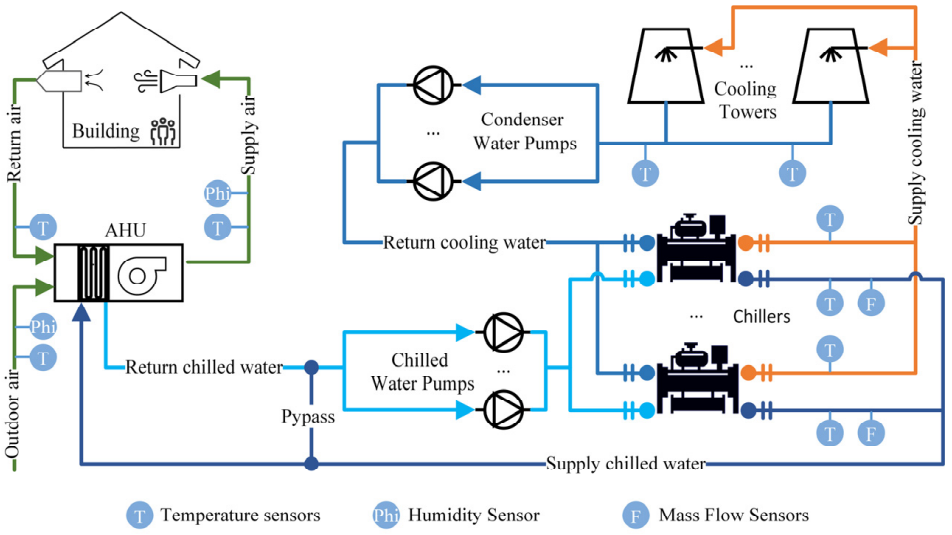

Figure 1. Diagram of a common HVAC system.

In addition, for the convenience of the following formulation and implementation of the optimization strategies, the system is controlled by a two-layer structure (as shown in Figure 2), including a supervisory layer and a control layer. The goal of the supervisory layer is to optimize the operation of the HVAC system and, while satisfying the cooling demand, reduce the system's energy consumption by adjusting setpoints of controllers. The control layer is responsible for the direct control of components from different parts of the system (for example, valves, and frequency converters), and this layer is also responsible for tracking given setpoints via the closed-loop feedback control (for example, the track of the chilled water supply temperature setpoint is achieved by the PID control of the chiller's compressor frequency). Under this control structure, direct open-loop optimization control of components is avoided, which ensures the stability of the system's operation [4].

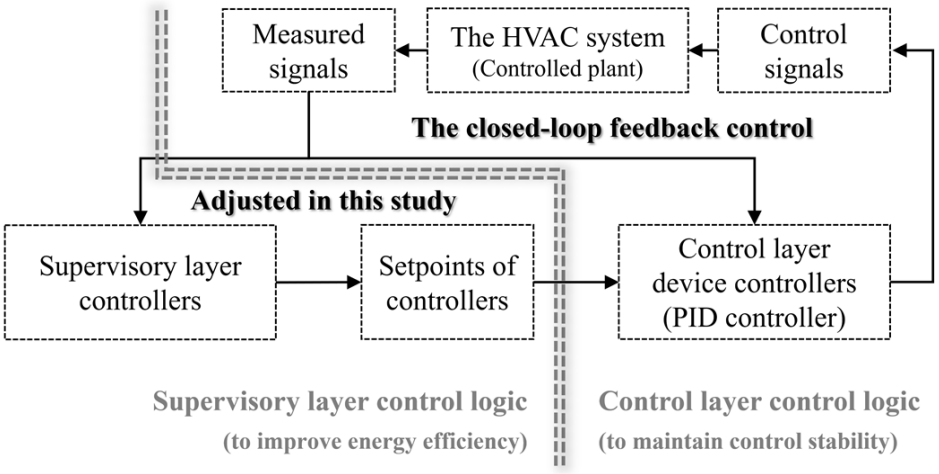

Figure 2. Diagram of the control structure.

Based on the above system, method for constructing training dataset was proposed, mainly including three steps as shown in Figure 3.

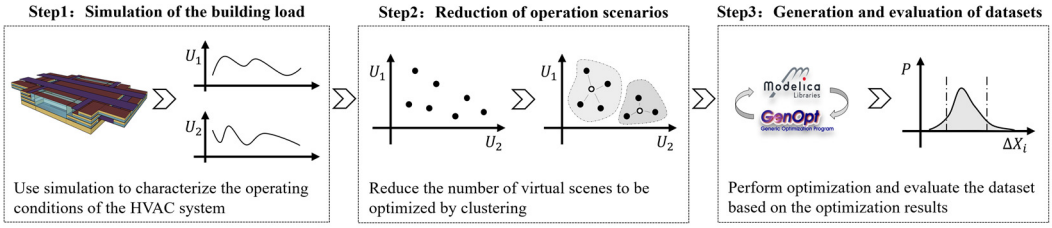

Figure 3. Method for constructing training dataset (U1 and U2 are descriptive variables of the system operation scenarios. There are more than two descriptive variables, but only two are shown in the diagram for the convenience of drawing).

2.1. Construction of Typical Operation Scenarios (Step1, Step2)

First of all, simulation of the system on the building's side was carried out throughout the cooling season, and the HVAC system's operation scenarios in time series are described by the simulated operation data. To ensure the accuracy and completeness of the simulated data, on the one hand, TMY (Typical Meteorological Year) file was taken as the weather boundary in simulation, so that all possible scenarios that may occur could be covered. On the other hand, in case some operation scenarios were left out due to long timestep, the simulation timestep was set to 10 min, which is relatively short. In addition, for the HVAC system shown in Figure 1, there are three disturbances affecting its operation: the outdoor dry-bulb temperature and outdoor relative humidity have an influence on the performance of cooling towers and air handling units; the cooling load determines the power of the equipment. Therefore, the three variables (the outdoor dry-bulb temperature, outdoor relative humidity, and the cooling load) were selected to describe the operation scenarios of the HVAC system.

Afterwards, the similarity of the sequential simulated operation scenarios was evaluated, and the simulated scenarios were clustered to reduce the number of typical operation scenarios. As mentioned earlier, the temporal correlation between scenarios does not need to be considered because there are no energy storage devices in the system, and only the correlation between different descriptive variables needs to be taken into account. First, the three descriptive variables were normalized. Then, the similarity of different operation scenarios was measured by Euclidean distance. The equations are as follows.

$$T'_{Out,i} = \frac{T_i - \min(T_{Out,1} \cdots T_{Out,n})}{\max(T_{Out,1} \cdots T_{Out,n}) - \min(T_{Out,1} \cdots T_{Out,n})} \tag{1}$$

$$Phi'_{Out,i} = \frac{Phi_{Out,i} - min(Phi_{Out,1} \cdots Phi_{Out,n})}{\max(Phi_{Out,1} \cdots Phi_{Out,n}) - min(Phi_{Out,1} \cdots Phi_{Out,n})} \tag{2}$$

$$Q'_{load,i} = \frac{Q_{load,i} - min(Q_{load,1} \cdots Q_{load,n})}{\max(Q_{load,1} \cdots Q_{load,n}) - min(Q_{load,1} \cdots Q_{load,n})} \tag{3}$$

$$d_{i,j} = \sqrt{\left(T'_{Out,i} - T'_{Out,j}\right)^2 + \left(Phi'_{Out,i} - Phi'_{Out,j}\right)^2 + \left(Q'_{load,i} - Q'_{load,j}\right)^2} \tag{4}$$

where $d_{i,j}$ represents the similarity of different scenarios, $T_{Out,1} \cdots T_{Out,n}$, $Phi_{Out,1} \cdots Phi_{Out,n}$ and $Q_{load,1} \cdots Q_{load,n}$, respectively, denotes outdoor dry-bulb temperature, outdoor relative humidity, and indoor cooling load.

In the last step, the K-means algorithm was used to cluster the simulated operation scenarios. This distance-based clustering algorithm can put scenarios with high similarity into one cluster. In addition, the center of each cluster was regarded as the typical operation scenario of this kind, and it represents all the operation scenarios in the cluster. Thus, the typical operation scenarios (namely the virtual operation scenarios to be optimized) were constructed.

2.2. Generation and Evaluation of the Training Dataset (Step3)

In the third step, model-based optimization was first used to calculate optimal setpoints of typical scenarios, and thus, the training dataset of the HVAC system was generated (The optimization method is described in detail in Section 3). Then, to evaluate the process of the dataset acquisition, the number of clusters, as the key parameter crucial to the efficiency of this process, was analyzed.

The rationality of the number of clusters can be judged by the difference of the optimal setpoints between adjacent typical operation scenarios. Figure 4 shows the change of the optimal setpoints when the number of clusters differs. U_1 and U_2 in the figure represents the descriptive variables of the typical scenarios, and X is the value of the optimal setpoint. As shown in the figure, when the number of clusters is too small, the similarity between adjacent typical operation scenarios is low, and the corresponding optimal setpoints also display large discrepancies (ΔX_1). In this case, each typical scenario includes too many operation scenarios, and the ideal optimal setpoints of these scenarios in one cluster differ greatly. Such differences are ignored and will affect the final implementation of the strategies. On the other hand, when the number of clusters is too large, the operation scenarios with high similarity are not well classified, resulting in a small difference in optimal setpoints between the adjacent typical scenarios (ΔX_2). The optimization of these typical scenarios does not bring much improvement on the implementation effect of strategies, and on the contrary, the efficiency of generating the training dataset declines if the number of clusters is too large.

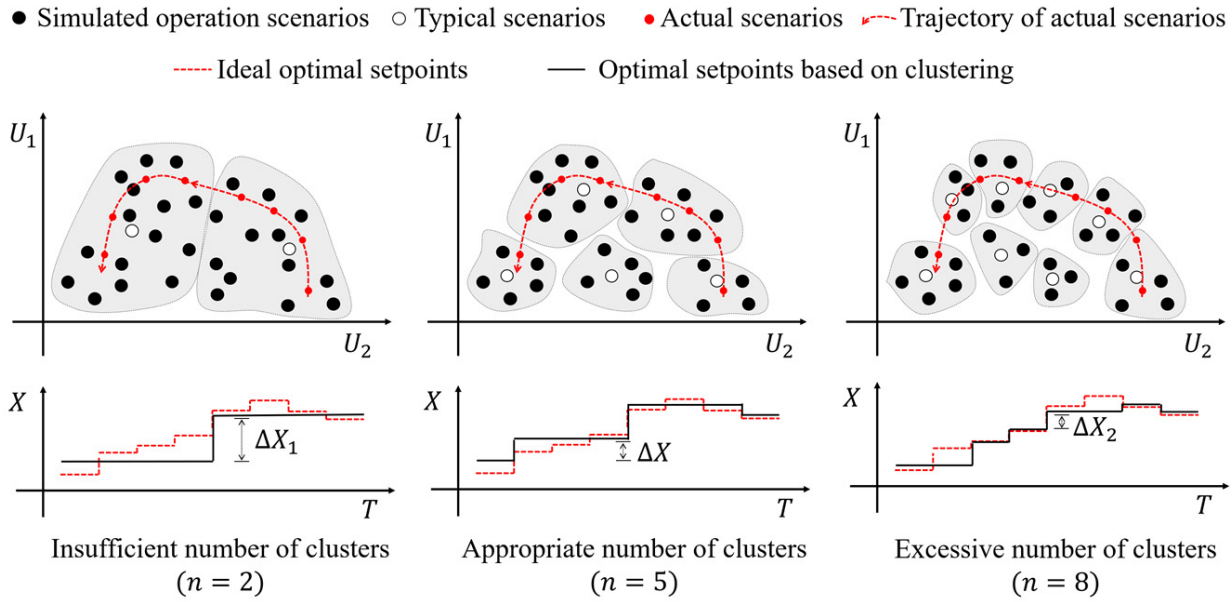

Figure 4. Optimal setpoints under different number of clusters.

The above discussion is based on one optimization variable, while HVAC systems often have multiple optimization variables. So, it is necessary to first determine how to calculate the difference of optimal setpoints between adjacent typical operation scenarios. Due to the complexity of searching for adjacent subspaces in a high-dimensional space, the adjacent subspaces (namely the adjacent operation scenarios) of one typical scenario were replaced by its similar operation scenarios. For a typical operation scenario, its adjacent scenarios are defined as the three other typical scenarios with the highest similarity to it. Moreover, as the optimization variables include both discrete and continuous ones, and the differences in the optimal value of discrete variables between similar scenarios also lead to large differences in the optimal value of continuous ones (e.g., the optimal water supply

temperature often varies greatly when different numbers of chillers are turned on.), the following calculation was designed:

$$Dif = \begin{cases} max\{\Delta U_{con,1}, \cdots, \Delta U_{con,i}\} & \nexists m \in [1,j] \ U_{dis,m} \neq U'_{dis,m} \\ max\left\{\Delta U_{dis,1}, \cdots, \Delta U_{dis,j}\right\} & \exists m \in [1,j] \ U_{dis,m} \neq U'_{dis,m} \end{cases} \quad (5)$$

$$\Delta U_{con,k} = \frac{\left|U_{con,k} - U'_{con,k}\right|}{2Acc_{con,k}} \quad k \in [1,i] \quad (6)$$

$$\Delta U_{dis,k} = \left|U_{dis,k} - U'_{dis,k}\right| \quad k \in [1,j] \quad (7)$$

where Dif indicates the difference between optimization results of similar typical operation scenarios (hereinafter referred to as the "difference index"), i and j, respectively, indicates the number of continuous optimization variables and discrete optimization variables, $U_{con,1\sim i}$ and $U_{dis,1\sim i}$, respectively, represents the value of continuous optimization variables and discrete optimization variables, and $Acc_{con,1\sim i}$ denotes the control accuracy of the optimization variables in the control system.

The distribution of the difference index was divided into three parts. Firstly, for the similar typical scenarios whose difference index is lower than the control accuracy of the control system ($Dif < 0.5$), it is difficult for the control system to differentiate the optimal setpoints of these similar scenarios, and thus the system operation cannot be optimized efficiently. Therefore, this region is called the inefficient optimization zone. The second part is where the difference index is higher than 1.5 ($Dif > 1.5$), and the similar typical scenarios in this region need to be further refined, because the optimal setpoints of these scenarios differ greatly and can be easily differentiated by the control system. The energy saving potential or even the operation of the system will be damaged if scenarios in this region are not further refined. The third part is called the efficient optimization region ($0.5 < Dif < 1.5$). In this region, smaller difference index means more details in the dataset and more energy saving for the system.

Based on the above analysis, the following three quantitative indicators were designed to evaluate the acquisition process of the training dataset:

$$Eff = 1 - \int_0^{0.5} f(Dif)dDif \quad (8)$$

$$Sta = 1 - \int_{1.5}^{+\infty} f(Dif)dDif \quad (9)$$

$$ESR = \int_{0.5}^{1.5} f(Dif)DifdDif \quad (10)$$

where $f(Dif)$ represents the probability density distribution of Dif; Eff represents the efficiency of acquiring the training dataset, and the value closer to one means higher efficiency; Sta denotes the reliability of the system's operation, and greater value means higher reliability; ESR denotes the energy saving effect, and smaller value means that more energy saving has been achieved.

3. Offline Optimization Framework

To verify the rationality and high efficiency of the method above for constructing the training dataset, an optimization framework was built (as shown in Figure 5) based on Coffey's framework [38,39]. The framework consists of two parts. One is for the offline optimization, and it calculates the optimal setpoints of the HVAC system under typical operation scenarios, thus generating the training dataset. The other part of the framework is for online implementation of strategies, which guides the operation of the actual system by the lookup table. Such an offline optimization framework is relatively simple. Moreover, by

applying the lookup table instead of using complex machine learning techniques to extract rules from the training dataset, excessive processing on the training dataset is avoided. Therefore, the quality of the training dataset can be directly reflected.

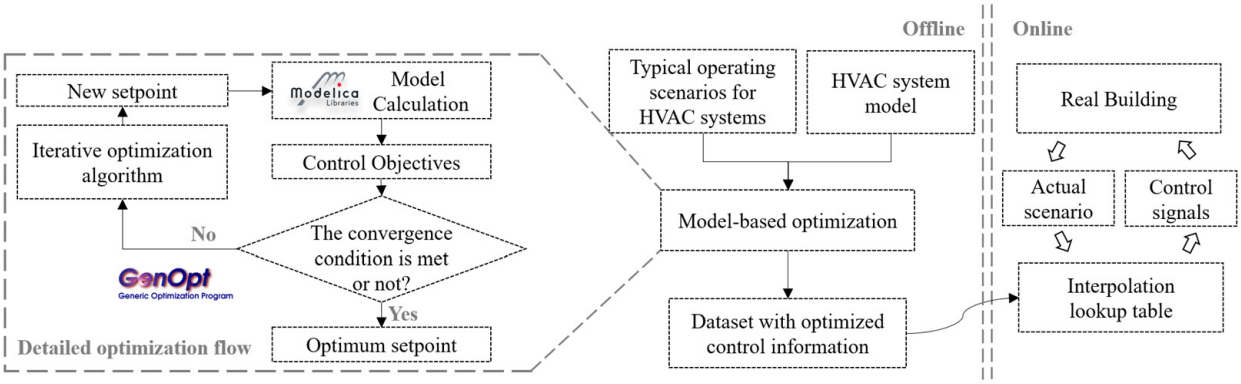

Figure 5. The diagram of the offline optimization framework.

In the offline optimization stage, the language Modelica was employed to establish the descriptive model (used for describing the relation between the setpoints and control strategies). Modelica is an object-oriented modeling language based on equations. It is suitable for modeling complex systems, and it can describe the constraints of the system (such as the frequency constraint) conveniently [9,40,41]. Then, GenOpt [42] was taken as the optimizer, and the optimal setpoints of different typical operation scenarios were obtained by optimization through iterative calls. The iterative computation process is shown in Figure 5. First, the model constructed using Modelica will calculate the optimal control objective (e.g., minimizing energy consumption). Then, GenOpt will determine whether the optimization problem satisfies the termination condition and if the optimum is not reached, GenOpt will calculate possible new sufficient setpoint values according to the optimization algorithm until the convergence condition is reached.

In the online implementation stage, the lookup table was employed, and Figure 6 shows how to use the lookup tables. After receiving the measured operation scenario of the HVAC system, the control system searches in the training dataset for a typical scenario with the highest similarity to the measured one, and then control the system with the corresponding optimal setpoints. This method has also been applied in [14,38].

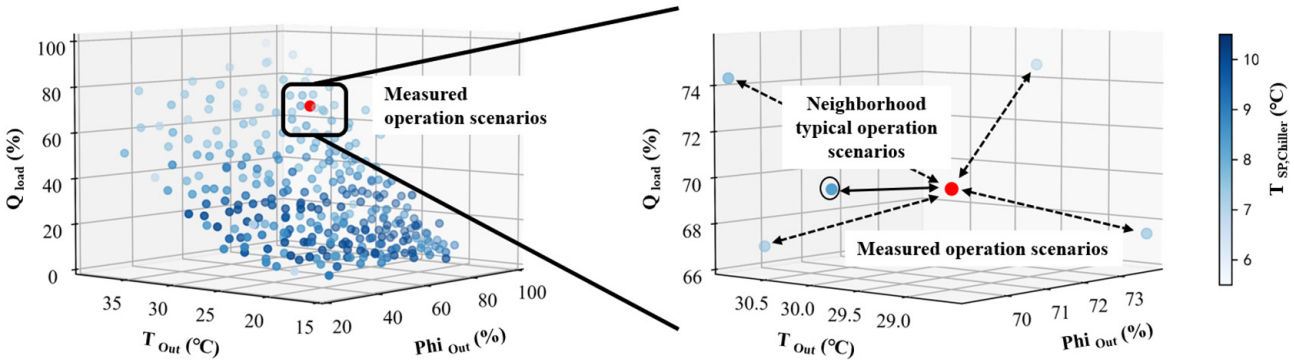

Figure 6. Diagram of searching for the optimal setpoints using the lookup table (The line between operation scenarios indicates the distance between similar scenarios, and the solid line connects the most similar combinations).

4. Research Case and Experimental Configuration

This section tests the methods proposed in this article using an actual engineering project as a case study. Section 4.1 introduces the basic situation of the case study, and Section 4.2 describes the relevant testing plans in conjunction with the testing content.

4.1. Case Description

The case study in this research is a high-speed railway station building (as shown in Figure 7) located in Beijing, China. The building is 36.50 m high and has four floors above ground (mainly for waiting areas), and three floors underground (for subways and transfer waiting areas). The subway air conditioning system provides the temperature and humidity environment control of the underground second and third floors and therefore is not considered in this research case. The configuration of the HVAC system is consistent with the one shown in Figure 1. Detailed information about the case is shown in Table 1. In addition, a combined air conditioning unit is mainly used to control the indoor environment, with a total cooling area of 322,000 square meters and a maximum cooling load of 43,718 kW.

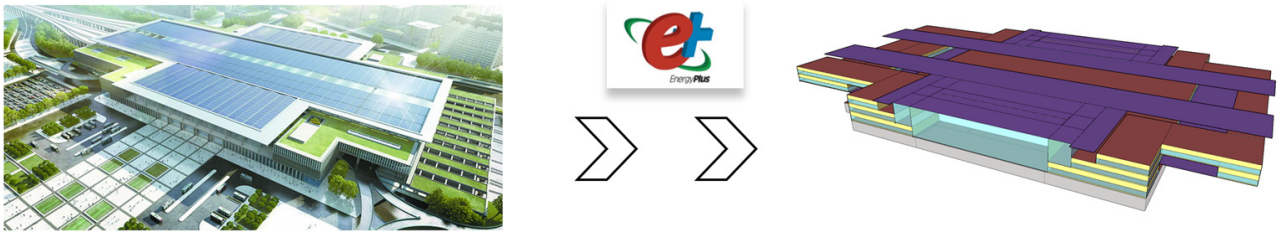

Figure 7. Building layout and EnergyPlus model.

Table 1. Detailed information about the study case.

Items	Parameters	Value
Building Construction and Occupancy	Wall conductivity Roof conductivity Window conductivity Heat gain coefficient of windows	0.34 W/(m^2k) 0.50 W/(m^2k) 2.2 W/(m^2k) 0.29 SHGC
	Window-to-Wall Ratio	East: 37% South: 35% West: 28% North: 37%
	Maximum occupancy	14,000 people
HVAC System	Chiller × 4	Nominal Capacity: 5630 kW IPLV: 9.364 Design COP: 6.030
	Chilled water pump × 4	Nominal flow rate: 1250 m^3/h Nominal head: 33 mH_2O Nominal speed: 980 r/min Nominal power: 160 kW
	Condenser water pump × 4	Nominal flow rate: 1250 m^3/h Nominal head: 33 mH_2O Nominal speed: 980 r/min Nominal power: 160 kW
	Cooling tower × 16	Nominal flow rate: 400 m^3/h Nominal power: 12 kW
Cooling demand	Indoor temperature Indoor relative humidity	27 °C <=70%

The HVAC system in this building employs a two-layer supervisory control structure. Table 2 displays the low-level control logic of each device and their original setpoints

outlined in the design document. The chiller's load is balanced based on load, meaning that the chiller's on/off sequence is determined by the load rate. The chiller is loaded when the load rate reaches 95% and unloaded when the surplus load rate of the activated chiller exceeds 105%.

Table 2. Control scheme for each equipment.

Plant	Control Variables	Equipment-Level Controls	Original Strategy
Cooling tower	$Num_{SP,Tower}$	On/Off control	1 chiller: 4 cooling towers *
	$T_{SP,Tower}$	PID control	$T_{Out,wet}$ + 4 °C
Condenser water pump	$Num_{SP,Pump,Con}$	On/Off control	1 chiller: 1 pump
	$\Delta T_{SP,Cool}$	PID control	5 °C
Chiller	$Num_{SP,Chiller}$	On/Off control	Load-based control
	$T_{SP,Chiller}$	PID control	6 °C
Chilled water pump	$Num_{SP,Pump,Chi}$	On/Off control	1 chiller: 1 pump
	$\Delta T_{SP,Chilled}$	PID control	7 °C
AHU	$T_{SP,SuAir}$	PID control	17 °C
	$T_{SP,Indoor}$	PID control	27 °C

* In the table, "1 chiller: 4 cooling towers" means the cooling towers are controlled by interlock, when one chiller is on, four cooling towers will be turned on.

4.2. Experimental Configuration

To comprehensively and accurately verify the effectiveness of the improved offline optimization framework, we constructed a simulation validation platform. The supervisory control is calculated by Python modules, while the dynamic operation process of the HVAC system is simulated by Modelica, thereby reflecting a more realistic control process of the system and the operating status of each device. The building's thermal dynamic model is constructed using EnergyPlus to achieve the most realistic feedback of indoor temperature and humidity. Different simulation tools are connected based on the FMI protocol [43].

On this validation platform, we aim to verify two aspects:

- Can the proposed method for constructing the training dataset in this paper support the offline optimization scheme and possess high computational efficiency?
- How does the number of clusters in the dataset acquisition stage influence the performance of system optimization, and can the verification included in the second section effectively reflect this influence?

To achieve this, we have designed experimental schemes as shown in Table 3, which were simulated for the same period of time (a complete cooling season from 1 May to 1 October) in the same meteorological boundaries (using typical year weather files) to compare the performance of different control strategies.

Complex optimization problems lead to higher verification and demonstration costs, and are not conducive to explaining the results. Therefore, each optimization group only optimizes 5 control variables: $T_{SP,Chiller}$, $Num_{SP,Chiller}$, $\Delta T_{SP,\ Chilled}$, $\Delta T_{SP,\ Cool}$, and $T_{SP,Tower}$, while other setpoint values are kept the same as the original values. The coexistence of discrete and continuous optimization variables ensures the representativeness of the demonstration. In the implementation process, to ensure the validity of the comparison, all experimental groups were configured with the same optimization algorithm (GPS-PSO optimization algorithm [42], the parameters were set as shown in Appendix A) and the same descriptive model (Figure 8). In addition, the impact of differences between the descriptive model and the actual system on the control effect is not the focus of this paper, so the HVAC system-side descriptive model used in the verification platform is consistent with the model used in the optimization.

Table 3. Experimental design.

Strategy	Source Literature	Detailed Explanations
Baseline Strategy (Base)	-	Use the original setpoints in the design data
Optimization Strategy 1 (Opt_A)	[17,19,34]	Use the time series of the full cooling season as the boundary and as a virtual scenario for sequential optimization simulation, and the control interval is chosen as 30 min
Optimization Strategy 2 (Opt_B)	-	Use the method mentioned in Section 2 (the number of clusters are selected as 400, 350, 300, 250, 200, 150, 100, 80, 60, 40, 20). The number of clusters is marked after the name for ease of writing (e.g., the optimization group 2 with the number of clusters 400 will be written as Opt_B_400)
Optimization Strategy 3 (Opt_C)	[38]	Using the orthogonal grid generation method to generate operational scenarios, where the grid interval is selected in the following way: • Outdoor dry bulb temperature: In 2 °C intervals, from 16 °C to 36 °C • Outdoor relative humidity: In 20% intervals, from 10% to 90% • Cooling load ratio: In 5% intervals, from 5% to 100%

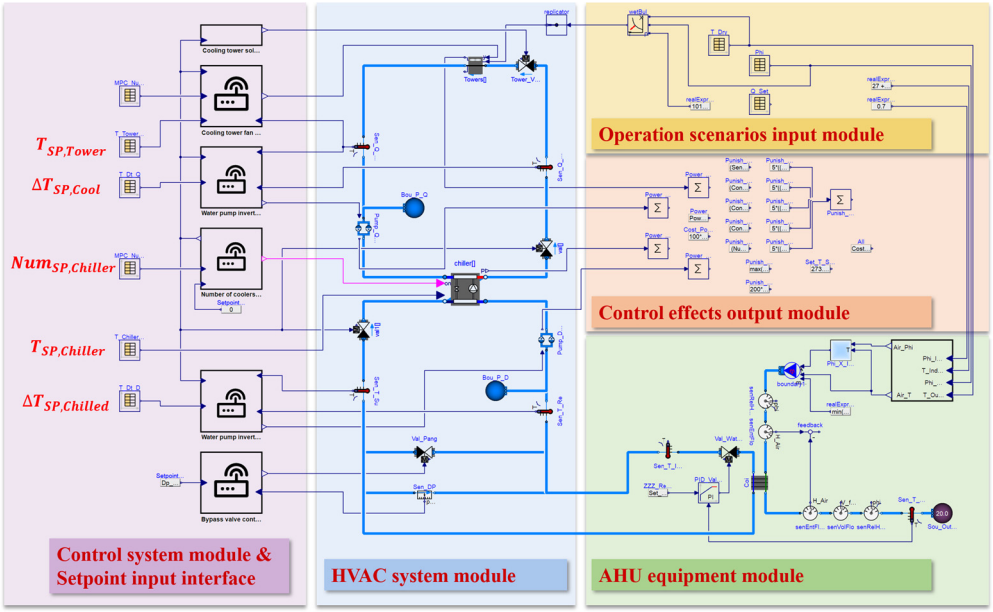

Figure 8. Diagram of the HVAC system model.

5. Results and Discussion

In this section, the validation results based on the research case are presented. The results are divided into three parts. Part 1 (Section 5.1) demonstrates the performance of the existing offline optimization scheme after applying the method for constructing the training dataset described in this paper. Part 2 (Section 5.2) compares the validation results of different optimization strategies to demonstrate and explain the efficiency of the method proposed in this paper. Part 3 (Section 5.3) shows the impact of the number of clusters on the final optimization and control performance, and it is used as a basis to explain the rationality of the validation process.

5.1. Optimized Control Effect Analysis

Satisfying the indoor cooling load demand is the prerequisite of optimal control, and to meet this prerequisite, we first analyzed the effect of indoor temperature and humidity control. We compared the offline optimization scheme with 400 clustering numbers (Opt_B_400) and the baseline strategy (Base), and Figure 9 shows the statistical results of indoor temperature and humidity distribution under the two schemes. The gray lines connect the temperature and humidity values of the two schemes at the same time points, and the slope of the lines can be used to judge the temperature and humidity changes for different schemes. It can be seen that throughout the cooling season, both the Base and Opt_B_400 groups exhibit similar indoor temperature and humidity control effects. The indoor temperature is controlled at around 27 °C for most of the time, and the relative humidity is controlled below 70%. The temperature and humidity values of the two schemes at the same time points are almost identical, indicating that the offline optimization scheme achieved the goal of indoor temperature and humidity control after applying the training dataset acquisition method proposed in this paper.

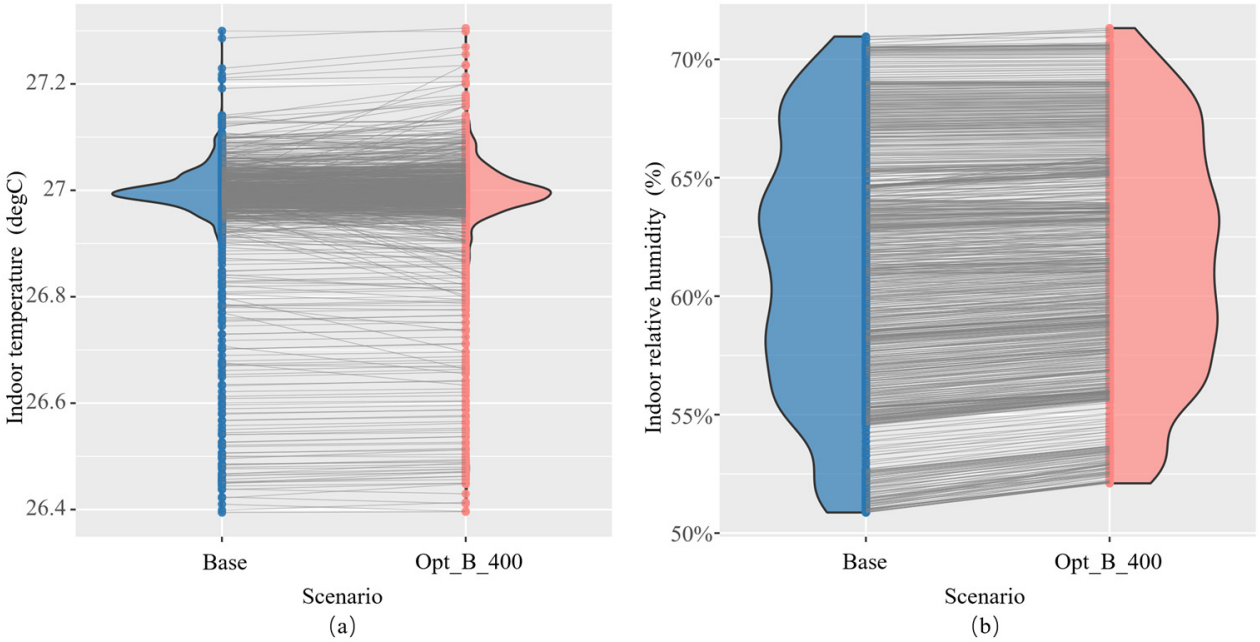

Figure 9. (**a**) Comparison of room temperature under two strategies; (**b**) Comparison of indoor relative humidity under two strategies. (In the figure, red represents the use of Opt_B_400 scheme, blue represents the use of Base scheme).

Reducing energy consumption is a primary goal of optimal control. Figures 10a and 10b, respectively, show the real-time power distribution and cumulative energy consumption of the two schemes, where the gray lines reflect the real-time power difference of the two schemes. From the figure, it can be observed that the gray lines connecting the Base group and the Opt_B_400 group show a downward trend. In terms of cumulative energy consumption, except for the cooling towers, the energy consumption of other equipment in the Opt_B_400 group is also lower to some extent. Additionally, calculations show that the Opt_B_400 group reduced overall energy consumption by 12.14% compared to the Base group. These pieces of evidence demonstrate that the method for acquiring the training dataset described in this paper can support the offline optimization framework to achieve the goal of reducing energy consumption.

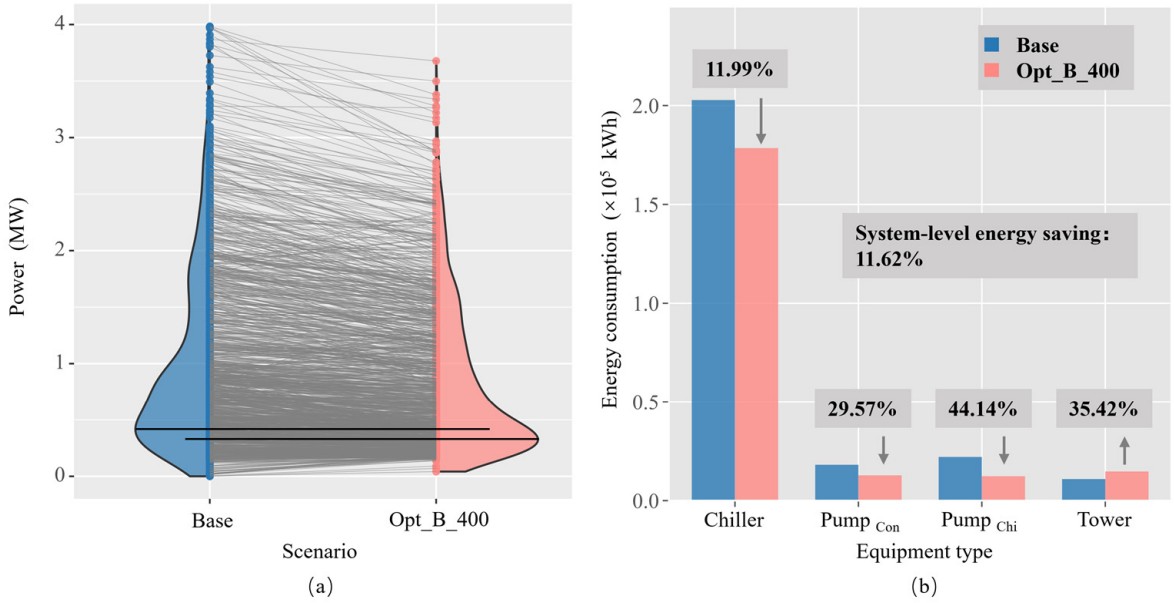

Figure 10. (**a**) Results of power comparison; (**b**) Comparison of cumulative electricity consumption by equipment type. (In the figure, red represents the use of Opt_B_400 scheme, blue represents the use of Base scheme).

5.2. Analysis of the Efficiency in Dataset Acquisition

Improving calculation efficiency of the optimization is the main research goal of this paper. Therefore, we compared the results of different optimization group to demonstrate the efficiency improvement of the pro-posed method. To ensure the completeness of the results, we calculated the energy saving rate, temperature setpoint non-guaranteed duration, and the computing time of offline optimization for each scheme. The energy saving rate is calculated based on the baseline strategy (Base), and when counting the non-guaranteed hours (when the room temperature control deviation is greater than 0.5 °C or relative humidity is above 70%), the non-guaranteed conditions shorter than 15 min were excluded to avoid errors caused by normal fluctuations. Table 4 shows the final results. The proposed method significantly reduces the workload in the strategy formulation phase compared to existing virtual scenario construction methods, thus achieving less computing time. At the same time, the energy saving rate has not changed much, and there is even some improvement in some scenarios (a decrease of only 0.44% compared to Opt_A, an increase of 0.12% compared to Opt_C). In addition, the non-guaranteed duration remains at a low level. These results demonstrate the efficiency improvement of the proposed method.

Table 4. Summary of simulated optimization results.

Strategy	Energy-Saving Rate	Non-Guaranteed Hours	Calculation Time/ Number of Optimizations Runs
Opt_A	12.06 %	5.9207 h	20.6106 d/5391 reps
Opt_C	11.50 %	8.2602 h	3.86439 d/1100 reps
Opt_B_400	11.62 %	7.0561 h	1.41498 d/400 reps

To better illustrate the efficiency of our proposed method and explain the reasons for the above results, we selected a typical day (20 July) from the entire cooling season for analysis. On this day, Opt_A and Opt_B_400 showed similar energy-saving effects (with energy-saving rates of 12.76% and 12.28%, respectively), but Opt_B_400 required 35% fewer optimization cycles than Opt_A (reduced from 48 cycles to 31 cycles), indicating that the clustering method effectively reduced the offline optimization workload.

Figure 11 shows the simulation optimization results for this day, where Figure 11a displays the meteorological conditions and cooling demand, and Figure 11b shows the variation of optimal setpoints on this day. The dark gray area in the graph represents the fact that Opt_B_400 treats the operation scenarios during this period as similar ones and therefore uses the same optimal setpoint for control. As can be seen from the figure, the trend of optimal setpoints in Opt_A and the trend in Opt_B_400 are quite similar on this day, which explains why they both exhibit similar energy-saving effects. In the dark gray area, the operation scenarios of the HVAC system have small variation and high similarity. The optimal setpoints in Opt_A vary within a limited range, while the optimal setpoints in Opt_B_400 remain constant because in the Opt_B_400 scheme, similar scenarios are treated as the same typical scenario. This also leads to the difference in the number of optimization process executions between the two schemes.

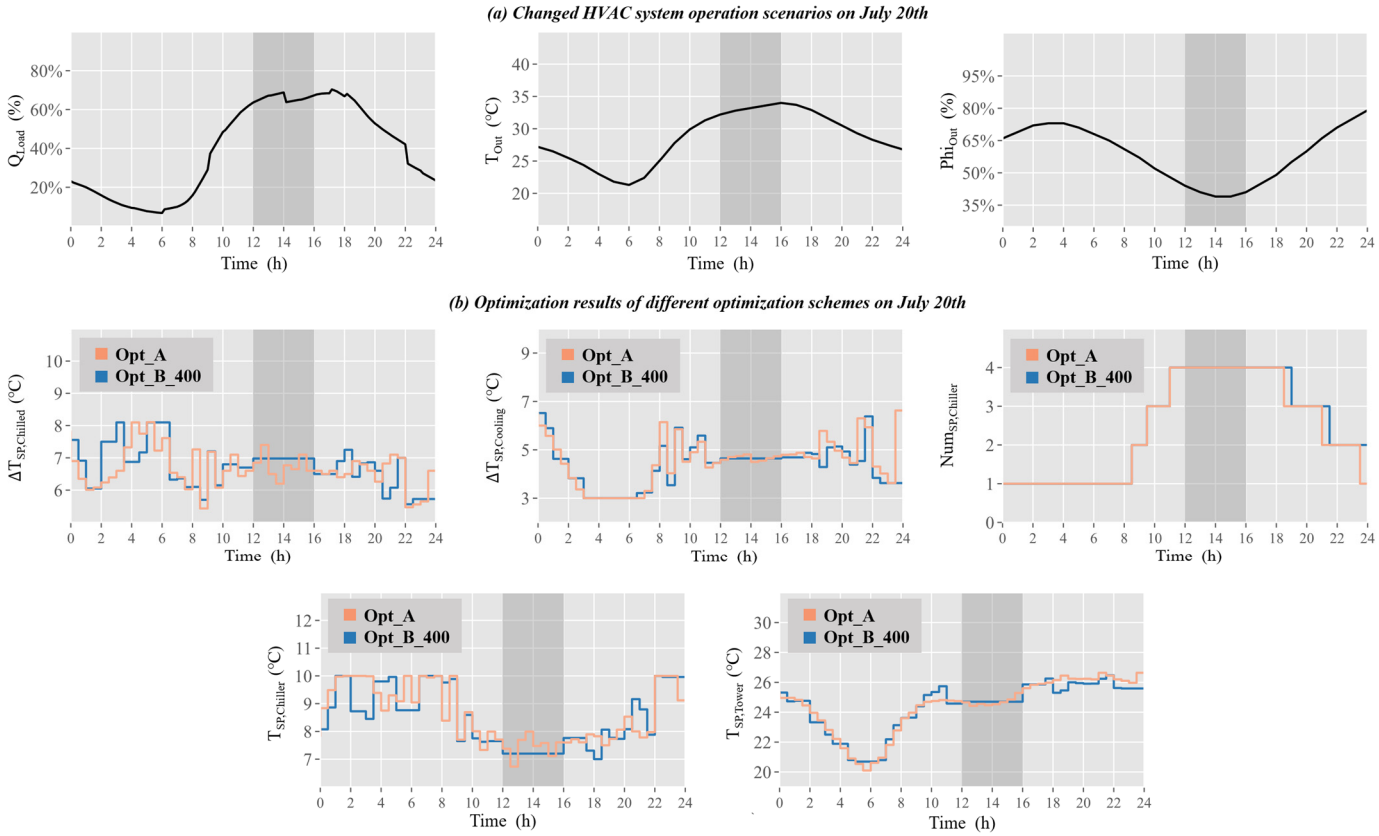

Figure 11. Simulation results under different optimization schemes on 20 July.

To investigate the effect of the clustering approach on the setpoints, we selected all the operation scenarios represented by the dark gray area in Figure 11 from the simulated data of the entire cooling season, and analyzed their setpoints. Figure 12 shows the composition of the operation scenarios before and after clustering, and the changes in the optimal setpoints under these scenarios. Part (a) shows the differences between typical operation scenarios and the similar scenarios that the typical ones represent, while Part (b) shows the differences in the optimal setpoints under these operation scenarios. From the figure, it can be seen that, on the one hand, the difference between typical operation scenarios and their similar scenarios is relatively small, with less than 1 °C in outdoor dry bulb temperature and less than 3% in both the outdoor relative humidity and cooling load ratio. On the other hand, the optimal setpoints for both types of scenarios also show certain similarities, with the difference in optimal setpoints for continuous variables within 1 °C and the optimal setpoints for discrete variables remaining consistent.

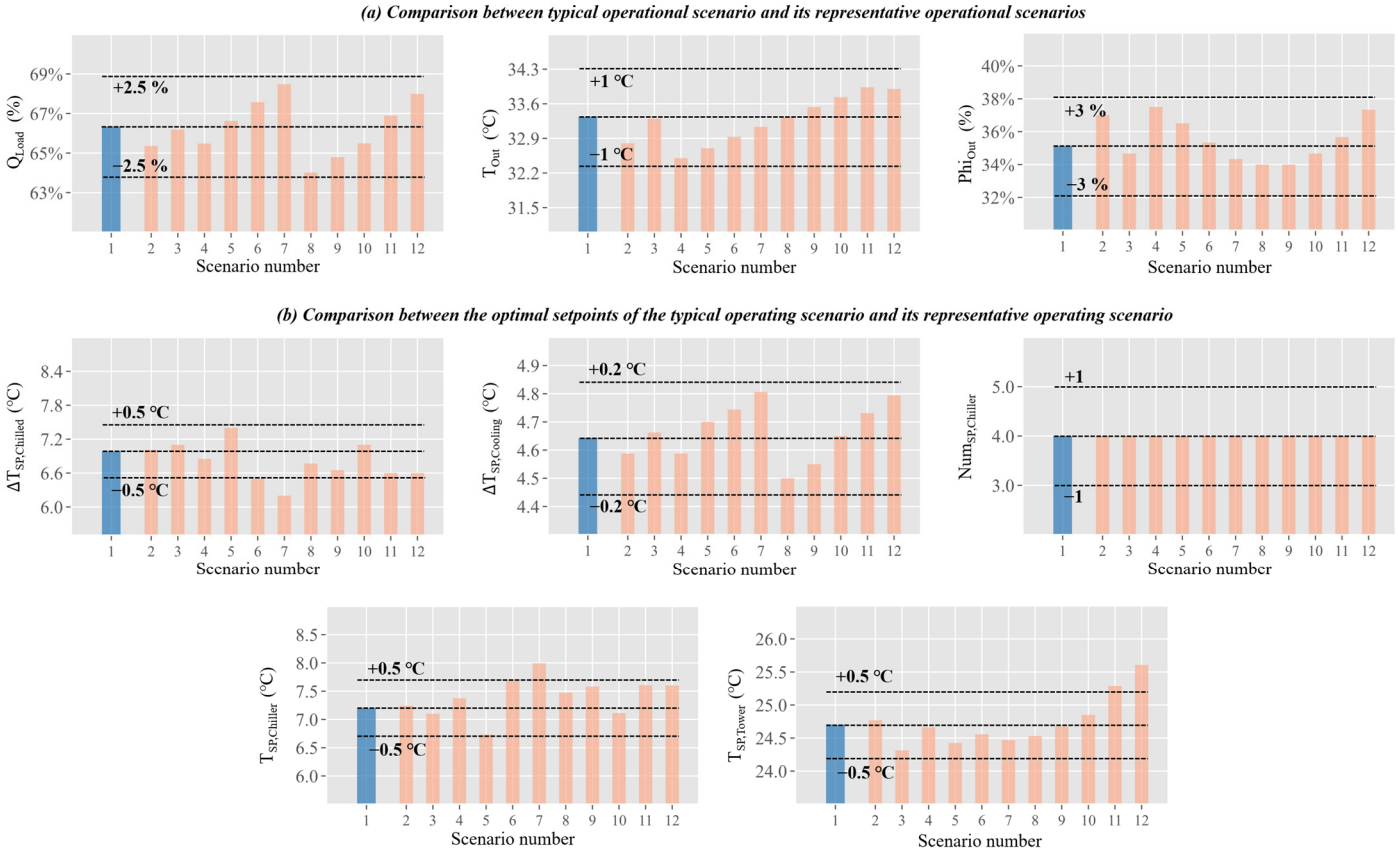

Figure 12. Analysis of optimal setpoints for typical and corresponding similar scenarios (blue bars represent typical operation scenarios, and orange bars represent the similar scenarios that the typical ones represent).

Finally, we analyzed the energy saving reduction caused by the changes in setpoints, and the results are shown in Figure 13. It can be seen that for these operation scenarios, the reduction in energy savings caused by using constant setpoints calculated from a typical operation scenario is limited (ranging from 0.02% to 1.02%) compared to optimizing each operation scenario individually with its corresponding optimal setpoints. In some operation scenarios (Scenario 7 and 8), there are even cases where Opt B has higher energy savings than Opt A, which is due to the local optima caused by the uncertainty of solution errors in the algorithm. Such results further demonstrate that reducing the number of operation scenarios does not have a significant impact on energy savings, which also confirms the validity of the method described in this paper.

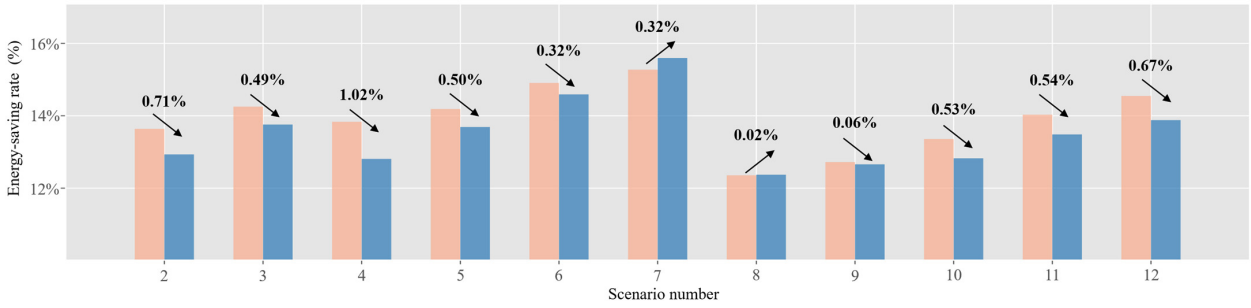

Figure 13. Comparison of energy-saving performance using different strategies in typical and corresponding similar scenarios (blue bars represent the fixed setpoint obtained from typical scenarios, orange bars represent the optimal setpoint obtained from similar scenarios).

5.3. Analysis of the Rationality of Evaluation Metrics

In the method for acquiring the training dataset described in this paper, more clusters mean more operation scenarios to be optimized, which can be beneficial for better results, but meanwhile, it also leads to longer calculation time for generating the training dataset. Selecting an appropriate number of clusters is crucial to improving the efficiency of dataset formulation, therefore, this paper added a verification step to the virtual scenario generation method to pre-judge the rationality of the number of clusters. To verify the effectiveness of this step, this section tests different number of clusters based on the case described in Section 4.

Figure 14 shows the test results, where Figure 14a presents the evaluation metrics calculated using the evaluation method described in Section 2, while Figure 14b shows the execution performance obtained through simulated operation on the virtual validation platform.

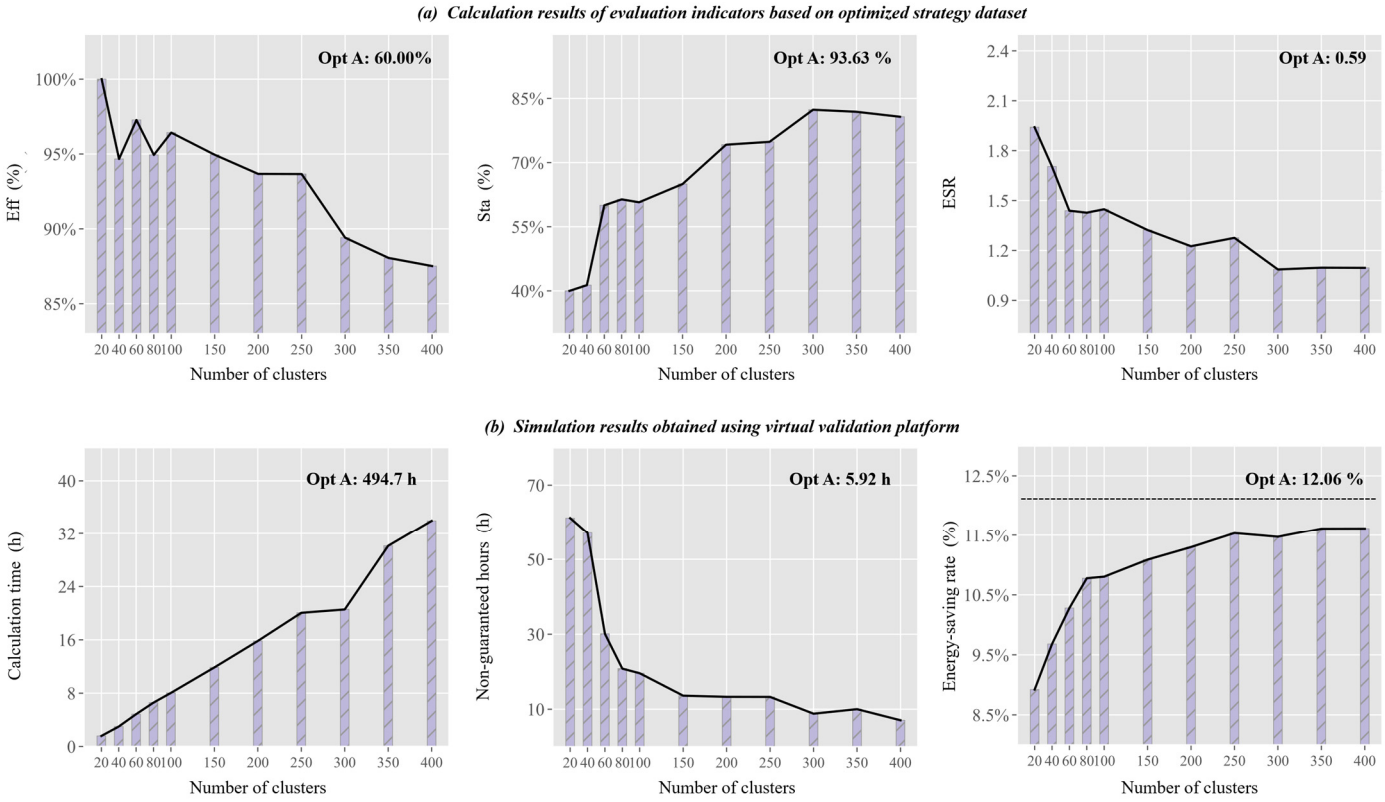

Figure 14. Changes of evaluation indicators and simulation results under different clustering numbers.

Firstly, for the dataset acquisition efficiency, there is a certain correlation between the Eff index (proportion of efficient optimization scenarios) and the calculation time. As the number of clusters increases, the Eff decreases and the calculation time increases. Secondly, for the indoor environment control effect, the Sta index (proportion of non-detailed scenarios) has a strong correlation with non-guaranteed hours throughout cooling season. As the number of clusters increases, the Sta gradually increases, and the non-guaranteed duration decreases, with both of their slopes showing a decreasing and stabilizing trend. Finally, for the evaluation of the system energy-saving effect, the change in the ESR index (average of the deviations from the optimal settings for similar scenarios) and the change in energy-saving rate throughout the full cooling season show a certain similarity. As the number of clusters increases, the former gradually decreases and the latter gradually increases, and both of their slopes gradually decrease.

These phenomena confirm the effectiveness of the validation process described in this paper. When virtual validation platforms are not available, the validation process included

in this method can effectively evaluate the training dataset. This is undoubtedly good news for the specification of optimization strategies.

In addition, in Figure 14, we have marked the corresponding indices of the opt A group in the upper right corner. It can be seen from the figure that although the computational efficiency of the proposed method may decrease when the number of clusters is selected to be large, it still maintains higher than that of the opt A group while ensuring a similar energy-saving rate. Therefore, in engineering applications, choosing the number of clusters as many as possible is an effective way to ensure the quality of the dataset.

6. Conclusions and Future Work

In this paper, we proposed a method of acquiring the training dataset to accelerate the process of generating optimal control strategies. The main idea is to avoid the inefficient optimization problem caused by similar scenarios when constructing the operation scenarios to be optimized. Therefore, we applied the clustering technique to process the operation scenarios. Additionally, we introduced a validation step to help designers to pre-evaluate the dataset's quality before dataset formulation.

We built a virtual simulation platform to test the proposed method in the case study. Compared to the standard method that uses the time-series data of the full cooling season as complete operation scenarios, the proposed method resulted in a 93.13% reduction in computing time with only a 0.45% loss in energy savings, demonstrating a significant improvement in the efficiency during dataset acquisition. The effectiveness of the validation step in this method was demonstrated by testing with different number of clusters. Additionally, quantitative results show that we can choose as many clusters as possible when using the methods described in this paper, which, although sacrificing some computational efficiency, can better support the development of the training dataset and lead to an increase in the quality of the dataset.

To the best of the author's knowledge, there are few studies on the acquisition of training datasets for the optimal control strategy generation process for HVAC systems. This research demonstrates the importance of this process for strategy extraction. However, this paper only analyzes and optimizes a relatively simple system, which has certain limitations. For the training dataset acquisition method, the following issues are worth further investigation in future studies:

1. This paper only considers the operation optimization of systems without energy storage where the temporal correlation between operation scenarios does not need to be paid much attention. However, when energy storage devices are involved, how to consider the temporal correlation between operation scenarios becomes a major issue.
2. The generation of the simulated operation scenarios to be optimized proposed in this paper is based on deterministic meteorological boundaries and occupancy patterns provided in design documents. However, in practical engineering, such information is often uncertain. Therefore, it is important to investigate how the differences between actual and design information impact the acquisition of the training datasets, especially when dealing with uncertain boundaries.

Author Contributions: Conceptualization, Z.T.; methodology, C.Y.; software, C.Y. and J.Z.; validation, C.Y. and J.N.; formal analysis, Z.T.; investigation, Z.T.; resources, Z.T.; data curation, Y.L. and C.Y.; writing—original draft preparation, C.Y.; writing—review and editing, Z.T. and J.N.; visualization, C.Y. All authors have read and agreed to the published version of the manuscript.

Funding: This research was funded by the Key R&D Program of Tianjin (22YFZCSN00180).

Conflicts of Interest: The authors declare no conflict of interest.

Nomenclature

Nomenclature	Description
T_{Out}	Outdoor dry-bulb temperature (°C)
Phi_{Out}	Outdoor relative humidity (%)
Q_{load}	Cooling load ratio (with maximum load as 100%) (%)
$\Delta T_{SP,\ Chilled}$	Setpoint of temperature difference between supply and return chilled water (°C)
$\Delta T_{SP,\ Cool}$	Setpoint of temperature difference between supply and return cooling water (°C)
$T_{SP,Chiller}$	Chiller outlet temperature setpoint (°C)
$T_{SP,Tower}$	Cooling tower outlet temperature setpoint (°C)
$T_{SP,SuAir}$	AHU supply air temperature setpoint (°C)
$T_{SP,Indoor}$	Indoor temperature setpoint (°C)
$Num_{SP,Chiller}$	Number of chillers in operation
$Num_{SP,Tower}$	Number of cooling towers in operation
$Num_{SP,Pump,Con}$	Number of condenser water pumps in operation
$Num_{SP,Pump,Chi}$	Number of chilled water pumps in operation

Appendix A. Setting Parameters of the Optimization Algorithm

Parameters	Value	Parameter	Value
Algorithm	GPSPSOCCHJ	CognitiveAcceleration	2.7
NeighborhoodTopology	vonNeumann	SocialAcceleration	1.3
NeighborhoodSize	5	MaxVelocityGainContinuous	0.5
NumberOfParticle	49	MaxVelocityDiscrete	4
NumberOfGeneration	20	ConstrictionGain	0.5

References

1. United Nations Environment Programme. *2021 Global Status Report for Buildings and Construction: Towards a Zero-Emission, Efficient and Resilient Buildings and Construction Sector*; United Nations Environment Programme: Nairobi, Kenya, 2021.
2. Pérez-Lombard, L.; Ortiz, J.; Pout, C. A review on buildings energy consumption information. *Energy Build.* **2008**, *40*, 394–398. [CrossRef]
3. *2019 Global Status Report for Buildings and Construction*; United Nations Environment Programme: Nairobi, Kenya, 2019; p. 41.
4. Wang, S.; Ma, Z. Supervisory and Optimal Control of Building HVAC Systems: A Review. *HVACR Res.* **2008**, *14*, 3–32. [CrossRef]
5. Drgoňa, J.; Arroyo, J.; Cupeiro Figueroa, I.; Blum, D.; Arendt, K.; Kim, D.; Ollé, E.P.; Oravec, J.; Wetter, M.; Vrabie, D.L.; et al. All you need to know about model predictive control for buildings. *Annu. Rev. Control* **2020**, *50*, 190–232. [CrossRef]
6. Serale, G.; Fiorentini, M.; Capozzoli, A.; Bernardini, D.; Bemporad, A. Model Predictive Control (MPC) for Enhancing Building and HVAC System Energy Efficiency: Problem Formulation, Applications and Opportunities. *Energies* **2018**, *11*, 631. [CrossRef]
7. Mariano-Hernández, D.; Hernández-Callejo, L.; Zorita-Lamadrid, A.; Duque-Pérez, O.; Santos García, F. A review of strategies for building energy management system: Model predictive control, demand side management, optimization, and fault detect & diagnosis. *J. Build. Eng.* **2021**, *33*, 101692. [CrossRef]
8. Nguyen, A.-T.; Reiter, S.; Rigo, P. A review on simulation-based optimization methods applied to building performance analysis. *Appl. Energy* **2014**, *113*, 1043–1058. [CrossRef]
9. Fu, Y.; Zuo, W.; Wetter, M.; VanGilder, J.W.; Han, X.; Plamondon, D. Equation-based object-oriented modeling and simulation for data center cooling: A case study. *Energy Build.* **2019**, *186*, 108–125. [CrossRef]
10. Merema, B.; Saelens, D.; Breesch, H. Demonstration of an MPC framework for all-air systems in non-residential buildings. *Build. Environ.* **2022**, *217*, 109053. [CrossRef]
11. Huang, S.; Zuo, W.; Sohn, M.D. Improved cooling tower control of legacy chiller plants by optimizing the condenser water set point. *Build. Environ.* **2017**, *111*, 33–46. [CrossRef]
12. Haves, P.; Hencey, B.; Borrell, F.; Elliot, J.; Ma, Y.; Coffey, B.; Sorin, B.; Michael, W. *Model Predictive Control of HVAC Systems: Implementation and Testing at the University of California, Merced*; Lawrence Berkeley National Lab.(LBNL): Berkeley, CA, USA, 2010. [CrossRef]
13. Campos, G.; Liu, Y.; Schmidt, D.; Yonkoski, J.; Colvin, D.; Trombly, D.M.; El-Farra, N.H.; Palazoglu, A. Optimal real-time dispatching of chillers and thermal storage tank in a university campus central plant. *Appl. Energy* **2021**, *300*, 117389. [CrossRef]
14. Granderson, J.; Lin, G.; Blum, D.; Earni, S.; Page, J.; Piette, M.A. Optimizing Operational Efficiency: Integrating Energy Information Systems and Model-Based Diagnostics. In *ESTCP Final Report: 201254*; Lawrence Berkeley National Laboratory: Berkeley, CA, USA, 2017.

15. Picard, D.; Jorissen, F.; Helsen, L. Methodology for Obtaining Linear State Space Building Energy Simulation Models. In Proceedings of the 11th International Modelica Conference, Versailles, France, 21–23 September 2015; pp. 51–58. [CrossRef]
16. May-Ostendorp, P.; Henze, G.P.; Corbin, C.D.; Rajagopalan, B.; Felsmann, C. Model-predictive control of mixed-mode buildings with rule extraction. *Build. Environ.* **2011**, *46*, 428–437. [CrossRef]
17. Domahidi, A.; Ullmann, F.; Morari, M.; Jones, C.N. Learning decision rules for energy efficient building control. *J. Process Control* **2014**, *24*, 763–772. [CrossRef]
18. Klaučo, M.; Drgoňa, J.; Kvasnica, M.; Cairano, S.D. Building Temperature Control by Simple MPC-like Feedback Laws Learned from Closed-Loop Data. *IFAC Proc. Vol.* **2014**, *47*, 581–586. [CrossRef]
19. Drgoňa, J.; Picard, D.; Kvasnica, M.; Helsen, L. Approximate model predictive building control via machine learning. *Appl. Energy* **2018**, *218*, 199–216. [CrossRef]
20. Afram, A.; Janabi-Sharifi, F. Review of modeling methods for HVAC systems. *Appl. Therm. Eng.* **2014**, *67*, 507–519. [CrossRef]
21. Wetter, M.; Wright, J. A comparison of deterministic and probabilistic optimization algorithms for nonsmooth simulation-based optimization. *Build. Environ.* **2004**, *39*, 989–999. [CrossRef]
22. Tang, R.; Wang, S. Model predictive control for thermal energy storage and thermal comfort optimization of building demand response in smart grids. *Appl. Energy* **2019**, *242*, 873–882. [CrossRef]
23. Kusiak, A.; Li, M.; Tang, F. Modeling and optimization of HVAC energy consumption. *Appl. Energy* **2010**, *87*, 3092–3102. [CrossRef]
24. Kusiak, A.; Xu, G. Modeling and optimization of HVAC systems using a dynamic neural network. *Energy* **2012**, *42*, 241–250. [CrossRef]
25. Afroz, Z.; Shafiullah, G.M.; Urmee, T.; Shoeb, M.A.; Higgins, G. Predictive modelling and optimization of HVAC systems using neural network and particle swarm optimization algorithm. *Build. Environ.* **2022**, *209*, 108681. [CrossRef]
26. Magnier, L.; Haghighat, F. Multiobjective optimization of building design using TRNSYS simulations, genetic algorithm, and Artificial Neural Network. *Build. Environ.* **2010**, *45*, 739–746. [CrossRef]
27. Perera, D.W.U.; Pfeiffer, C.F. Control of temperature and energy consumption in buildings—A review. *Energy Environ.* **2014**, *5*, 471–484.
28. Afram, A.; Janabi-Sharifi, F. Theory and applications of HVAC control systems—A review of model predictive control (MPC). *Build. Environ.* **2014**, *72*, 343–355. [CrossRef]
29. Baños, R.; Manzano-Agugliaro, F.; Montoya, F.G.; Gil, C.; Alcayde, A.; Gómez, J. Optimization methods applied to renewable and sustainable energy: A review. *Renew. Sustain. Energy Rev.* **2011**, *15*, 1753–1766. [CrossRef]
30. Sun, F.; Yu, J.; Zhao, A.; Zhou, M. Optimizing multi-chiller dispatch in HVAC system using equilibrium optimization algorithm. *Energy Rep.* **2021**, *7*, 5997–6013. [CrossRef]
31. Gao, Z.; Yu, J.; Zhao, A.; Hu, Q.; Yang, S. Optimal chiller loading by improved parallel particle swarm optimization algorithm for reducing energy consumption. *Int. J. Refrig.* **2022**, *136*, 61–70. [CrossRef]
32. Zheng, Z.; Li, J.; Duan, P. Optimal chiller loading by improved artificial fish swarm algorithm for energy saving. *Math. Comput. Simul.* **2019**, *155*, 227–243. [CrossRef]
33. Chen, S.; Liu, X.; Fu, H. Design of Energy-saving Optimized Remote Control System of Chiller Based on Improved Particle Swarm Optimization. In Proceedings of the 2018 5th IEEE International Conference on Cloud Computing and Intelligence Systems (CCIS), Nanjing, China, 23–25 November 2018; pp. 299–304. [CrossRef]
34. Kusiak, A.; Xu, G.; Zhang, Z. Minimization of energy consumption in HVAC systems with data-driven models and an interior-point method. *Energy Convers. Manag.* **2014**, *85*, 146–153. [CrossRef]
35. Castilla, M.; Álvarez, J.D.; Normey-Rico, J.E.; Rodríguez, F. Thermal comfort control using a non-linear MPC strategy: A real case of study in a bioclimatic building. *J. Process Control* **2014**, *24*, 703–713. [CrossRef]
36. Åkesson, J.; Årzén, K.-E.; Gäfvert, M.; Bergdahl, T.; Tummescheit, H. Modeling and optimization with Optimica and JModelica.org—Languages and tools for solving large-scale dynamic optimization problems. *Comput. Chem. Eng.* **2010**, *34*, 1737–1749. [CrossRef]
37. Drgona, J.; Helsen, L.; Vrabie, D.L. Cutting the Deployment Costs of Physics-Based MPC in Buildings by Simulation-Based Imitation Learning. In Proceedings of the ASME 2020 Dynamic Systems and Control Conference, Virtual, 5–7 October 2020. [CrossRef]
38. Coffey, B. Approximating model predictive control with existing building simulation tools and offline optimization. *J. Build. Perform. Simul.* **2013**, *6*, 220–235. [CrossRef]
39. Coffey, B.; Haghighat, F.; Morofsky, E.; Kutrowski, E. A software framework for model predictive control with GenOpt. *Energy Build.* **2010**, *42*, 1084–1092. [CrossRef]
40. Wetter, M.; Zuo, W.; Nouidui, T.; Pang, X. Modelica Buildings library. *J. Build. Perform. Simul.* **2014**, *7*, 253–270. [CrossRef]
41. Wetter, M.; Treeck, C.; Helsen, L.; Maccarini, A.; Saelens, D.; Robinson, D.; Schweiger, G. IBPSA Project 1, BIM/GIS and Modelica framework for building and community energy system design and operation—Ongoing developments, lessons learned and challenges. *IOP Conf. Series Earth Environ. Sci.* **2019**, *323*, 012114. [CrossRef]

42. Wetter, M. GenOpt®—A Generic Optimization Program. In Proceedings of the Seventh International IBPSA Conference, Rio de Janeiro, Brazil, 13–15 August 2001.
43. Hatledal, L.I.; Zhang, H.; Collonval, F. Enabling Python Driven Co-Simulation Models with PythonFMU. In Proceedings of the ECMS 2020 Proceedings; Communications of the ECMS, Berlin, Germany, 9–12 June 2020; Volume 34.